Proceedings of FEDSM'03
4TH ASME_JSME Joint Fluids Engineering Conference
Honolulu, Hawaii, USA, July 6–11, 2003

FEDSM2003-45006

THERMAL CAVITATION EXPERIMENTS ON A NACA 0015 HYDROFOIL

Emilio Rapposelli
Research Engineer, CENTROSPAZIO – Consorzio Pisa Ricerche
Via A. Gherardesca, 56121 Pisa, Italy

Angelo Cervone
Ph.D. Student, Dipartimento di Ingegneria Aerospaziale
Via G. Caruso, 56126 Pisa, Italy

Cristina Bramanti
Ph.D. Student, Dipartimento di Ingegneria Aerospaziale
Via G. Caruso, 56126 Pisa, Italy

Luca d'Agostino
Professor, Dipartimento di Ingegneria Aerospaziale, Università di Pisa
Via G. Caruso, 56126 Pisa, Italy

ABSTRACT

The present paper illustrates the main results of an experimental campaign conducted in the Thermal Cavitation Tunnel of the CPRTF (Cavitating Pump Rotordynamic Test Facility) at Centrospazio. Experiments were carried out on a NACA 0015 hydrofoil at various incidence angles, cavitation numbers and freestream temperatures, in order to investigate the characteristics of cavitation instabilities and the impact of thermal cavitation effects. Measured cavity length, surface pressure coefficients and unsteady pressure spectra are in good agreement with the data available in the open literature and suggest the existence of a strong correlation between the onset of the various forms of cavitation and instabilities, the thermal cavitation effects, and the effects induced by the presence of the walls of the tunnel. Further analytical investigations will be carried out in order to provide a better interpretation of the above results.

INTRODUCTION

Propellant feed turbopumps are a crucial component of all primary rocket propulsion concepts powered by liquid propellant engines because of the severe limitations associated with the design of high power density, dynamically stable machines capable of meeting the extremely demanding suction, pumping and reliability requirements of space transportation systems. In these systems cavitation is the major source of performance degradation of the turbopump and provides the necessary flow excitation and compliance for triggering dangerous rotordynamic and/or fluid mechanic instabilities of the machine or the entire propulsion system (POGO auto-oscillations). In addition, in cryogenic fluids close to saturation conditions thermodynamic phenomena are known to represent the dominant source of cavitation scaling effects.

As a rough initial approximation, the cavitating behavior of a rotating machine can be related to that of a static cascade of hydrofoils; so, the first step for understanding cavitation instabilities and thermodynamic scaling effects is typically represented by experimentation on test bodies in hydrodynamic tunnels.

Cavitation instabilities on hydrofoils are generated by fluctuations of the cavity length caused by the inherent unsteady nature of the flow and the interaction with the pertinent boundary conditions. Franc (2001) distinguishes two classes of instabilities: *system* instabilities, in which the unsteadiness comes from the interaction between the cavitating flow and the rest of the system (inlet and outlet lines, tanks, valves), and *intrinsic* instabilities, whose features, such as frequency content, are independent from the rest of the system.

The most known example of system instability is represented by cavitation surge, sometimes observed in supercavitating hydrofoils (Wade & Acosta, 1966) as a result of the extreme sensitivity of long cavities to external pressure fluctuations generated by other components of the circuit.

On the other hand, a typical example of intrinsic instability is the so-called "cloud cavitation". When a sheet cavity on a hydrofoil attains a certain size, it starts a violent periodical oscillation, releasing a cloud cavity downstream at each cycle: Kubota et al. (1989), using laser Doppler anemometry with a conditional sampling technique, showed that the shed cloud consists of a large-scale vortex containing a cluster of many small bubbles. The intrinsic nature of this form of instability has been largely elucidated: experiments carried out in various facilities of different characteristics and hydraulic impedances, or in adjustable configurations of the same facility (Tsujimoto, Watanabe & Horiguchi, 1998), lead to very similar Strouhal numbers for cloud oscillations. Further investigations have proved the correlation between cloud cavitation and the re-

entrant jet generated at the cavity closure as a result of a critical adverse pressure gradient observed for cavity lengths greater than about 50% of chord (Callenaere, Franc & Michel, 1998; Kawanami, Kato, Yamaguchi, Tagaya & Tanimura, 1997; Sakoda, Yakushiji, Maeda & Yamaguchi, 2001).

Thermal cavitation effects on hydrofoils have been extensively investigated in the past. Kato et al. (1996) observed a temperature depression along the cavity, which becomes more significant when freestream temperature increases. At different freestream temperatures, cavities with comparable lengths were found to have comparable thickness, but could be observed at different cavitation numbers (bigger for higher temperatures). The conclusion drawn by Kato and his collaborators was that the reference length scale of thermodynamic cavitation effect must be the separated layer thickness at the leading edge of the cavity. Tani & Nagashima (2002) compared the cavitation behavior of a NACA 0015 hydrofoil in water and in cryogenic fluids, showing the important role of the cavity Mach number, different in the two cases because of the different sound speeds.

Yet, a number of aspects of unsteady flow phenomena in cavitating turbopumps and hydrofoils, including their connection with thermal cavitation effects, are still partially understood and imperfectly predicted by theoretical means alone. Technology progress in this field must therefore heavily rely on detailed experimentation on scaled models. To this purpose Centrospazio has developed a low-cost instrumented facility, the CPRTF, Cavitating Pump Rotordynamic Test Facility (Rapposelli, Cervone & d'Agostino, 2002). The inlet section of the facility has been recently reconfigured allowing for the installation of a Thermal Cavitation Tunnel, TCT (Rapposelli, Cervone, Bramanti & d'Agostino, 2002), where current experiments have been conducted.

NOMENCLATURE

c	chord length
C_p	pressure coefficient
f	frequency
L_{cav}	cavity length
p	pressure
p_{in}	hydrofoil upstream pressure
p_V	vapor pressure
Re	Reynolds number
St	Strouhal number
T	freestream temperature
V	freestream velocity
α	incidence angle
ν	kinematic viscosity
ρ	density
σ	cavitation number

EXPERIMENTAL APPARATUS

The CPRTF (Figure 1) has been designed for general experimentation on noncavitating/cavitating turbopumps and test bodies in water under fluid dynamic and thermal cavitation similarity. It has been specifically intended for investigating rotordynamic fluid forces in forced vibration experiments on turbopumps with rotors of adjustable eccentricity and sub-synchronous or super-synchronous whirl speeds.

The alternative CPRTF configuration used in the present experimentation is the Thermal Cavitation Tunnel, specifically designed for analyzing 2D or 3D cavitating flows over test bodies. In this configuration the pump is simply used to generate the required mass flow.

Figure 1. CPRTF with the pump test section (left) and the Thermal Cavitation Tunnel mounted on the suction line.

The test body, a NACA 0015 hydrofoil with 115mm chord and 80mm span length, is mounted on a blind panel on the bottom of the rectangular test section (120x80x500mm). Optical access is allowed through three large Plexiglas windows located on the lateral and top sides of the test section.

Figure 2 shows a schematic of the test section, with the hydrofoil instrumented with 12 pressure taps, 10 on the suction side and 2 on the pressure side. Three taps are located on the bottom panel upstream and 3 downstream of the test section to monitor the inlet/outlet pressure. The incidence angle can be manually adjusted as necessary for the specific experiment.

The tunnel maximum velocity is 8 m/s and the Reynolds number ($\mathrm{Re} = c \cdot V / \upsilon$) is maintained higher than $5 \cdot 10^5$ in the following tests. The freestream temperature is measured by a digital thermometer mounted inside the water tank. Water is heated by a 5 kW electrical resistance from room conditions to a maximum of 90 °C.

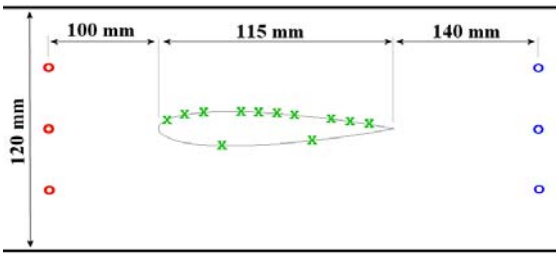

Figure 2. Schematic of the test section with the NACA 0015 hydrofoil and the locations of the pressure taps on the hydrofoil surface (x), at the section inlet (o) and outlet (o).

RESULTS AND DISCUSSION

Pressure coefficient

The present experimental tests have been conducted to analyze the pressure coefficient in noncavitating and inertial/thermal cavitating conditions on the suction side of the NACA 0015 hydrofoil. During these experiments pressure was measured at each pressure tap for constant values of the tunnel velocity, water temperature, incidence angle and cavitation number $\sigma = (p_{in} - p_V) \Big/ \frac{1}{2}\rho V^2$.

In particular, Figure 3 shows the pressure coefficient profile in noncavitating conditions for different incidence angles at room water temperature. As expected, the experimental results are different from the surface pressure distribution in unconstrained flow. The lateral constraints to the flow pattern promote "solid blockage" with the increase of the dynamic pressure, the hydrofoil forces and moments at given incidence angle (Kubota, Kato & Yamaguchi, 1992).

The results have been also compared with a CFD simulation in order to validate the numerical code developed for noncavitating/cavitating flows around 2D or 3D test bodies. The data presented in the figure refer to simulations at 8° incidence angle under constrained conditions. Experimental results are in good agreement with the numerical reconstructions.

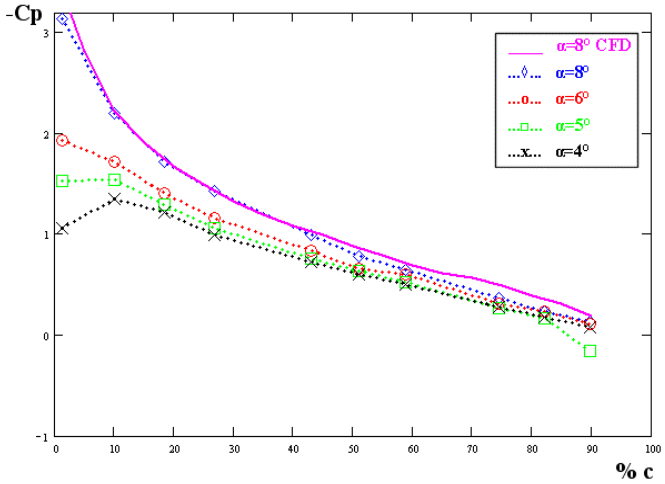

Figure 3. Pressure coefficient on the suction side of the NACA 0015 hydrofoil in noncavitating conditions for various incidence angles α at room water temperature. CFD simulation at 8° incidence angle and room water temperature (solid line).

Figure 4 compares the pressure profiles in cavitating conditions for three different freestream water temperatures at the same cavitation number and incidence angle. At higher temperatures the absorption of the latent heat at the cavity interface increases, reducing the vapor pressure under the unperturbed saturation value. This trend is well reflected in the figure: at 70 °C, due to pressure decrement under saturation value, the pressure recovery occurs more upstream than at room temperature.

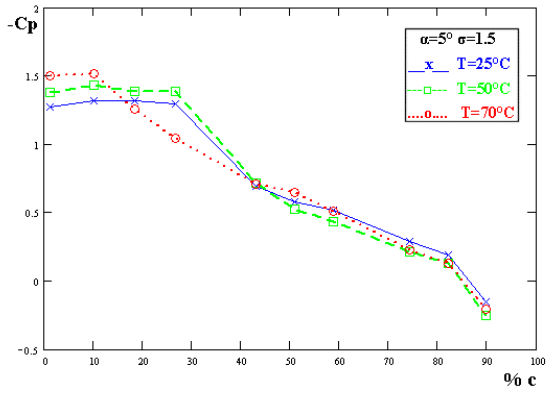

Figure 4. Influence of thermal cavitation effects on surface pressure distribution on the NACA 0015 hydrofoil at constant angle of attack α and cavitation number σ for several water temperatures T.

Cavity oscillations

A number of experiments have been carried out in order to determine the characteristics of the cavity length and oscillations at different incidence angles, cavitation numbers and freestream temperatures. Cavity length for each nominal condition was calculated by taking pictures of the cavitating hydrofoil at a frame rate of 30 fps, during a period of 1 second. Mean cavity length along the span was determined for each picture with a maximum estimated error of 4% of the chord length. As a final result of this process, maximum, minimum and mean value of the 30 cavity lengths were obtained. At the same time, frequency spectrum of the upstream pressure was measured in each flow condition.

Figure 5 shows the maximum and minimum cavity lengths for various incidence angles at room water temperature. The cavity length and the frequency spectrum of the upstream pressure are shown in Figures 6 and 7 for the case of 8° incidence angle and room water temperature.

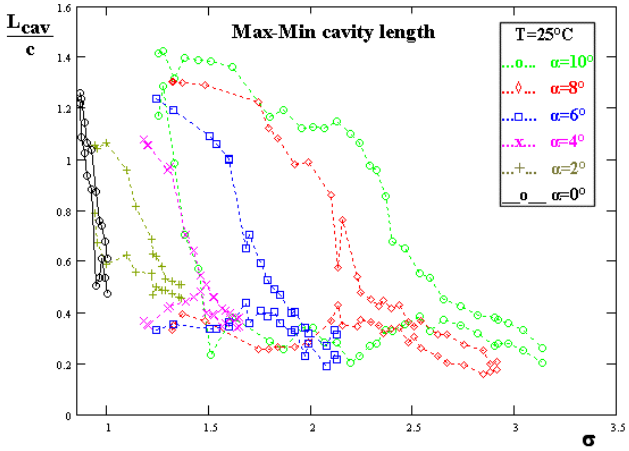

Figure 5. Normalized maximum and minimum lengths of the cavity as function of the cavitation number σ for various incidence angles α at room water temperature.

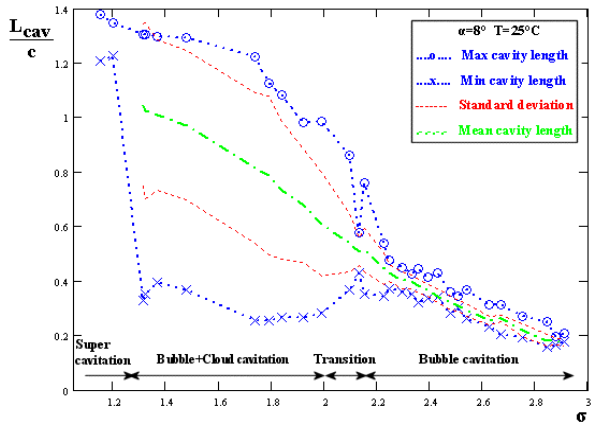

Figure 6. Characteristics of cavity length at 8° incidence angle and room water temperature.

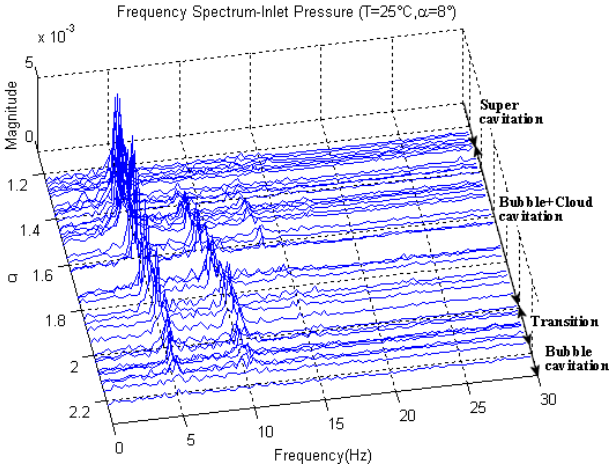

Figure 7. Frequency spectrum of the upstream pressure at 8° incidence angle and room water temperature.

Analysis of Figures 6 and 7 shows that the maximum and minimum cavity lengths provide a good qualitative indication of cavitation behavior on the hydrofoil at different cavitation numbers. One can recognize three different regimes of cavitation, corresponding to different ranges of values of σ:

- Supercavitation ($\sigma < 1.3$): both minimum and maximum cavity lengths are larger than the chord length. There are practically no cavity oscillations and therefore the frequency spectrum is almost flat.
- Bubble+Cloud cavitation ($1.3<\sigma<2$): the flow pictures show the occurrence of an initial zone of bubbly cavitation, followed by a second zone where the bubbles coalesce and strong cloud cavitation oscillations are observed. The frequency of these oscillations is almost constant at different cavitation numbers with a Strouhal number ($St = f \cdot c / V$) of about 0.2, similar to those obtained by Tsujimoto et al. (1998) and Kjeldsen et al. (1998). Other frequencies, multiple of the first, are present in the spectrum. One can speculate that the second frequency might be related to the second, faster re-entrant jet sometimes observed by Sakoda et al. (2001). More likely, since higher frequencies are integer multiples of the fundamental one, they may be the result of the frequency spreading caused by nonlinear effects in the flow field.
- Bubble cavitation ($\sigma>2.1$): after a short transition zone, cloud cavitation disappears. Only the traveling bubble cavitation zone remains, with drastically reduced pressure oscillations (flat frequency spectrum).

Figure 8 shows the typical aspect of cavitation in "Bubble+Cloud" case for a particular experimental condition.

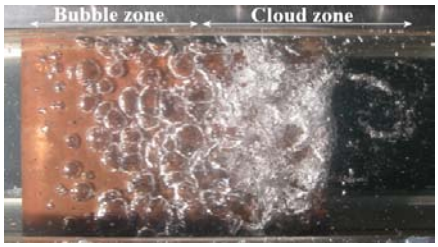

Figure 8. Typical cavitation appearance in "Bubble+Cloud" case ($\alpha = 4°, \sigma = 1.25, T = 25°C$).

Thermal cavitation tests were carried out with a similar procedure for 8° incidence angle at two different freestream temperatures (50 °C and 70 °C). Results are shown in Figures 9,10 and 11.

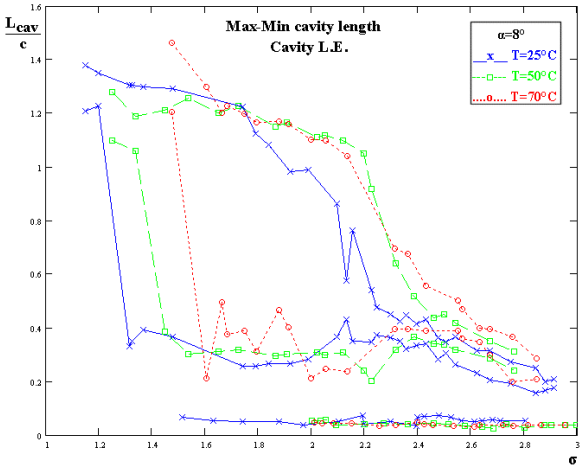

Figure 9. L.E., maximum and minimum lengths of the cavity for three different water temperatures T at 8° incidence angle.

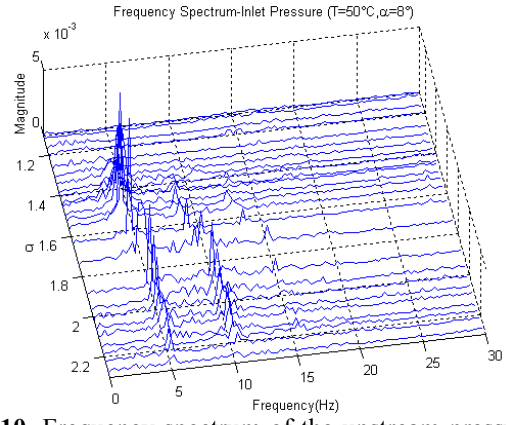

Figure 10. Frequency spectrum of the upstream pressure at 8° incidence angle and 50 °C water temperature.

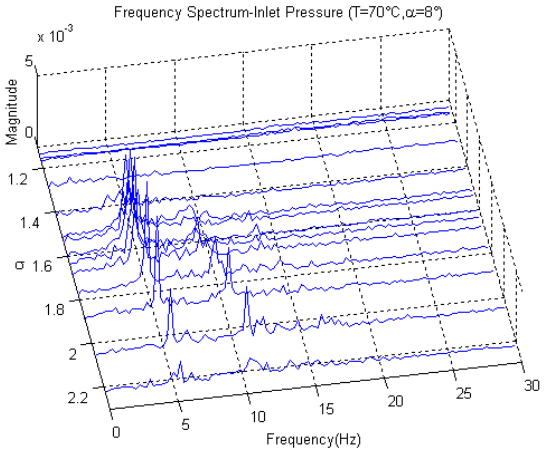

Figure 11. Frequency spectrum of the upstream pressure at 8° incidence angle and 70 °C water temperature.

Figures show that, for higher freestream temperatures, the "Bubble+Cloud cavitation" zone tends to spread over a wider range of cavitation numbers and to begin at higher values of σ. Similarly, supercavitation also begins at higher cavitation numbers. These findings are in accordance with the results obtained by Kato et al. (1996), who compared the temperature depressions in the cavity in water tests at 120 °C and 140 °C.

At higher freestream temperatures and constant cavitation number, the cavity tends to become thicker and longer, even when there are no oscillations ("Bubble cavitation" zone), as shown in Figure 12.

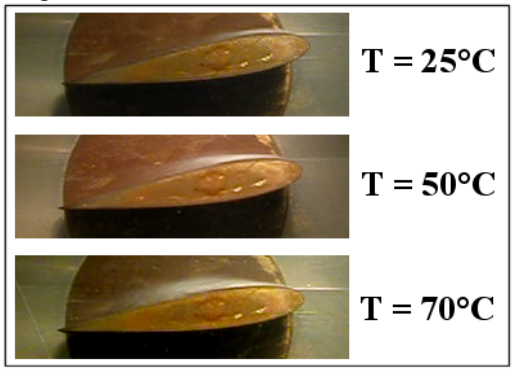

Figure 12. Cavity thickness for three different water temperatures T at the same incidence angle α and cavitation number σ $(\alpha = 8°, \sigma = 2.5)$.

Figure 13. Cavitation appearance at higher freestream temperature $(\alpha = 8°, \sigma = 2, T = 70°C)$.

The above results can be explained by the increased compliance of the cavity, which is strictly related to the decrease of the cavity Mach number at higher temperatures. The "solid blockage" effect can also play an important role in the process, by increasing the flow velocity and lowering the pressure. Cavitation at higher freestream temperatures looks quite different: bubbles are smaller and tend to coalesce more easily, resulting in a narrower and less defined "bubble zone" compared to the "cloud zone" (Figure 13).

Thermal effects on the pressure drop

Another set of experiments was conducted in order to determine the pressure drop caused by the hydrofoil at various incidence angles, freestream temperatures and cavitation numbers. Tests were performed using a differential pressure transducer mounted between one of the pressure taps upstream of the test body and the corresponding pressure tap downstream. The pressure drop obtained using this procedure represents therefore a "punctual" value that cannot be directly related to the drag, but should nevertheless exhibit a similar general behavior. Figures 14 and 15 show, respectively, the results obtained for different incidence angles and for the same incidence angle at different freestream temperatures.

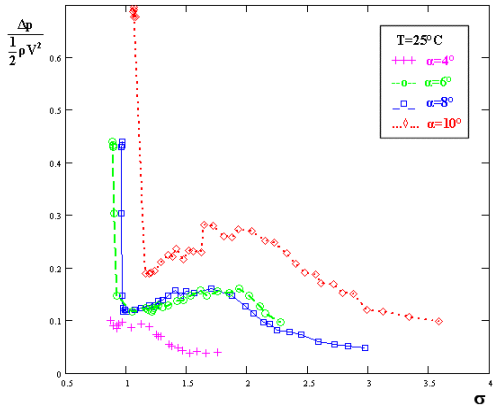

Figure 14. Normalized pressure drop caused by the hydrofoil for various incidence angles α at room water temperature.

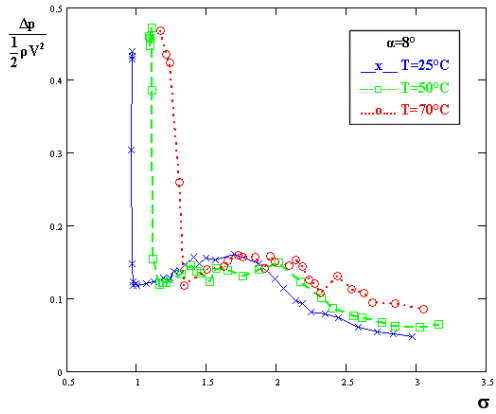

Figure 15. Normalized pressure drop caused by the hydrofoil for three different water temperatures T at 8° incidence angle.

The figures show a sudden rise of the pressure drop for cavitation numbers slightly smaller than those corresponding to the onset of supercavitation; at higher freestream temperatures this "breakdown" effect occurs at higher cavitation numbers, just like supercavitation and cloud cavitation oscillation.

This behavior, strictly related to the increase of cavity thickness (Figure 12), is different from that observed on hydrofoils in free flows and in cascades, probably as a result of the more significant "solid blockage" effect (in a free flow there is no solid blockage, in a staggered cascade solid blockage is less effective because the blades overlap only partially).

CONCLUSIONS

A number of experiments were carried out on a NACA 0015 hydrofoil in order to investigate the correlation between the onset of the various forms of cavitation and instabilities, the thermal cavitation effects and the wall effects. The main results of the investigation are:

- At increasing values of the cavitation number three different cavitation zones develop: supercavitation, bubble+cloud cavitation and bubble cavitation. Each zone corresponds to a different behavior of the upstream pressure frequency spectrum.
- At higher freestream temperatures, both cloud cavitation oscillation and supercavitation begin at higher cavitation numbers and, for the same cavitation number, cavity tends to become thicker and longer.
- The sudden rise of the pressure drop caused by the hydrofoil shifts towards higher cavitation numbers at higher freestream temperatures, as a consequence of the retarded onset of supercavitation.

The last two results could be explained taking into account the interaction between the greater compliance of the cavity and the "solid blockage" effect caused by the tunnel walls, more significant with respect to hydrofoils in free flows and cascades.

Further analytical investigations are planned in order to provide a better interpretation of the above results.

ACKNOWLEDGEMENTS

The realization of the CPRTF has been jointly supported by the European Space Agency under the FESTIP-1 contract No. 11.482/95/NL/FG and by the Agenzia Spaziale Italiana under the 1998 and 1999 contracts for fundamental research. The development of the Thermal Cavitation Tunnel was funded by the program FAST2 (Italian national technology program for future space launchers) in collaboration with CIRA (Centro Italiano Ricerche Aerospaziali).

The authors would like to acknowledge the help of the students F. d'Auria, S. Bondi, D. Mazzini, R. Menoni, L. Vigiani and A. Milani, who participated to the design of the facility, and express their gratitude to Profs. Mariano Andrenucci and Renzo Lazzeretti of the Dipartimento di Ingegneria Aerospaziale, Università degli Studi di Pisa, Pisa, Italy, for their constant and friendly encouragement.

REFERENCES

Callenaere M., Franc J.P., Michel J.M., 1998, "Influence of Cavity Thickness and Pressure Gradient on the Unsteady Behaviour of Partial Cavities", *3rd International Symposium on Cavitation*, Grenoble, France, April 7-10

Franc J.P., 2001, "Partial Cavity Instabilities and Re-Entrant Jet", *CAV2001, Int. Symposium on Cavitation*, Pasadena, California, USA, June 20-23.

Kawanami Y., Kato H., Yamaguchi H, Tagaya Y. & Tanimura M., 1997, "Mechanism and control of cloud cavitation", *J. of Fluids Eng.*, Vol. 119, pp. 788-795

Kawanami Y., Kato H. & Yamaguchi H., 1998, "Three-dimensional characteristics of the cavities formed on a two-dimensional hydrofoil", *3rd International Symposium on Cavitation*, Grenoble, France, April 7-10

Kato H., Maeda M., Kamono H. & Yamaguchi H., 1996, "Temperature Depression in Cavity", *Fluids Engineering Division Conference*, San Diego, USA, July 7-11

Kjeldsen M., Effertz M. & Arndt R.E.A., 1998, "Investigation of Unsteady Cavitation Phenomena", *Proc. of US-Japan Seminar: Abnormal Flow Phenomena in Turbomachinery*, Osaka, Japan, Nov. 1-6

Kubota A., Kato H., Yamaguchi H. & Maeda M., 1989, "Unsteady structure measurement of cloud cavitation on a foil section using conditional sampling technique", *J. of Fluids Eng.*, Vol. 111, pp. 204-210

Kubota A., Kato H. & Yamaguchi H., 1992, "A new modelling of cavitating flows: a numerical study of unsteady cavitation on a hydrofoil section", *J. Fluid Mech.*, Vol. 240, pp. 59-96

Rapposelli E., Cervone A. & d'Agostino L., 2002, "A New Cavitating Pump Rotordynamic Test Facility", *JPC, AIAA Joint Propulsion Conference and Exhibit*, Indianapolis, USA, July 7-10

Rapposelli E., Cervone A., Bramanti C. & d'Agostino L., 2002, "A New Cavitation Test Facility at Centrospazio", *4th International Conference on Launcher Technology*, Liege, Belgium, December 3-6

Sakoda M., Yakushiji R., Maeda M., Yamaguchi H., 2001, "Mechanism of Cloud Cavitation Generation on a 2-D Hydrofoil", *CAV2001, Int. Symposium on Cavitation*, Pasadena, California, USA, June 20-23.

Tani N. and Nagashima T., 2002, "Numerical Analysis Of Cryogenic Cavitating Flow On Hydrofoil – Comparison Between Water and Cryogenic Fluids", ", *4th International Conference on Launcher Technology*, Liege, Belgium, December 3-6

Tsujimoto Y., Watanabe S. & Horiguchi H., 1998, "Linear Analyses of Cavitation Instabilities of Hydrofoils and Cascades", *Proc. of US-Japan Seminar: Abnormal Flow Phenomena in Turbomachinery*, Osaka, Japan, Nov. 1-6

Wade R.B. and Acosta A.J., 1966, "Experimental Observations on the flow past a plano-convex hydrofoil", *J. of Basic Engineering*, Vol. 87, pp. 273-283

